# Half-life and excitation energy of the $I^{\pi} = 13/2^{+}$ isomer in $^{209}$Ra

K. Hauschild,[1] A. Lopez-Martens,[1] A. V. Yeremin,[2] O. Dorvaux,[3] A. V. Belozerov,[2] M. L. Chelnokov,[2] V. I. Chepigin,[2] B. Gall,[3] V. A. Gorshkov,[2] M. Guttormsen,[4] P. Jones,[5] A. P. Kabachenko,[2] A. Khouaja,[3] A. C. Larsen,[4] O. N. Malyshev,[2] A. Minkova,[6,7] H. T. Nyhus,[4] Yu. Ts. Oganessian,[2] D. Pantelica,[8] A. G. Popeko,[2] F. Rotaru,[8] S. Saro,[9] A. V. Shutov,[2] S. Siem,[4] A. I. Svirikhin,[2] and N. U. H. Syed[4]

[1]*CSNSM, IN2P3-CNRS, F-91405 Orsay Campus, France*
[2]*FLNR, JINR, Dubna, Russia*
[3]*IPHC, IN2P3-CNRS, F-67037 Strasbourg, France*
[4]*Department of Physics, Oslo University, N-0316 Oslo, Norway*
[5]*Accelerator Laboratory, University of Jyväskylä, P. O. Box 35, FIN-40351, Finland*
[6]*Department of Atomic Physics, University of Sofia, B-1164 Sofia, Bulgaria*
[7]*INRNE (Institute for Nuclear Research and Nuclear Energy), Bulgarian Academy of Sciences, 72 Tsarigradsko chaussee, B-1784 Sofia, Bulgaria*
[8]*Institute for Physics and Nuclear Engineering, Bucharest Magurele, P. O. Box MG6, Romania*
[9]*Department of Physics, Comenius University, SK-84215, Bratislava, Slovakia*
(Received 29 January 2008; published 29 April 2008)

An isomeric state in $^{209}$Ra has been observed for the first time, using the GABRIELA setup at the focal plane of VASSILISSA, to decay to the ground state of $^{209}$Ra via a cascade of 238-keV ($M2$) and 644-keV transitions. The half-life of the isomer has been measured to be 117(5) $\mu$s and from systematics is assigned as a neutron $i^{-1}_{13/2}$ excitation.

DOI: 10.1103/PhysRevC.77.047305 PACS number(s): 27.80.+w, 23.35.+g, 23.20.Lv, 23.20.Nx

In the region around $^{208}$Pb the relatively low number of valence protons and neutrons provides an ideal laboratory to test the shell model. In particular, valuable information on nuclear structure and nucleon-nucleon interactions can be obtained due to the relative purity of isomeric states. The lowest lying unique parity states in odd-$A$ nuclei in this region are often isomeric which facilitates their observation. In this Brief Report a previously unobserved isomer in $^{209}$Ra was studied.

Excited states in $^{209}$Ra were populated using the fusion-evaporation reaction $^{174}$Yb($^{40}$Ar,5$n$) at a nominal midtarget beam energy of 192 MeV. The $Yb_2O_3$ target had an isotopic enrichment of 98.1%, a thickness of 350 $\mu$g/cm$^2$ and was mounted on a 1.5 $\mu$m Ti backing. The ∼30 pnA $^{40}$Ar beam was provided by the U400 cyclotron of the FLNR, JINR, Dubna and the total beam dose accumulated during this ∼160 min irradiation was $1.59 \times 10$ particles. Fusion-evaporation residues were transported by the VASSILISSA separator [1,2] and implanted into a 16-strip position sensitive Si detector of the GABRIELA setup [3]. A combined time-of-flight and energy measurement allowed the evaporation residues (ERs) to be distinguished from the background of scattered beam and transfer products. The subsequent time- and position-correlated $\alpha$ decays of the implanted ERs were also measured in the Si implantation detector in anti-coincidence with the time-of-flight detectors. An in-beam energy calibration was performed with the following known $\alpha$ decays [5]: $^{210}$Rn $E_{\alpha} = 6040(2)$ keV, $^{210}$Fr $E_{\alpha} = 6543(5)$ keV, $^{214}$Ra $E_{\alpha} = 7137(3)$ keV, $^{214}$Ac $E_{\alpha} = 7214(5)$ keV, $^{215}$Ac $E_{\alpha} = 7604(5)$ keV, and $^{215}$Ra $E_{\alpha} = 8699(5)$ keV, which were populated by bombarding $^{197}$Au and $^{198}$Pt targets with $^{22}$Ne.

Four 4-strip Si detectors, placed upstream of the implantation detector in a tunnel configuration, were used to detect conversion electrons emitted in the backward direction by the implanted nuclei and their daughter products. Using the $^{184}$W($^{22}$Ne,5$n$) reaction $^{201}$Po was produced and implanted into the focal plane detector. An isomeric $I^{\pi} = 13/2^{+}$ level, at an excitation energy of 424 keV, has a 56% branch decaying via a 418-keV $M4$ transition [6]. In addition, the sequence $^{201}\mathrm{Po} \overset{EC}{\rightarrow} {}^{201}\mathrm{Bi} \overset{EC}{\rightarrow} {}^{201}\mathrm{Pb}$ populates a similar $13/2^{+}$ state that decays by a 629-keV $M4$ transition. In this way, the electron calibration for the tunnel detectors could be corrected for the energy losses in the implantation detector.

Seven germanium detectors from the French-UK loan pool were used to detect $\gamma$-rays emitted from the ERs and their daughters. Six of these detectors were Compton suppressed.

The signals from all detectors were processed individually and time-stamped with a 1 $\mu$s precision when written to hard disk. Events were subsequently constructed during the off-line analysis.

The total alpha spectrum obtained during this measurement is shown in Fig. 1(a). In this mass region the decay properties of many neighboring nuclei are very similar; for example the alpha decay energies of $^{209}$Ra and $^{210}$Ra are 7008(5) and 7018(5) keV, and their half-lives are 4.6(2) and 3.7(2) s, respectively [4]. From these data we obtained $E_{\alpha} = 7007(4)$ keV [with a full width at half maximum = 27 keV (FWHM)] and a total of 6825(83) $\alpha$-particles detected for the doublet labeled $^{209/210}$Ra.[1] The inset, (b), presents a plot of the time difference measured between the implantation of an

[1]Since the optical parameters for VASSILISSA were tuned during this run, a measurement of the reaction cross section is not possible. However, from similar runs we estimate the $4n + 5n$ ($^{210,209}$Ra) cross section to be of the order of $\sigma \sim 150$ $\mu$b.

 

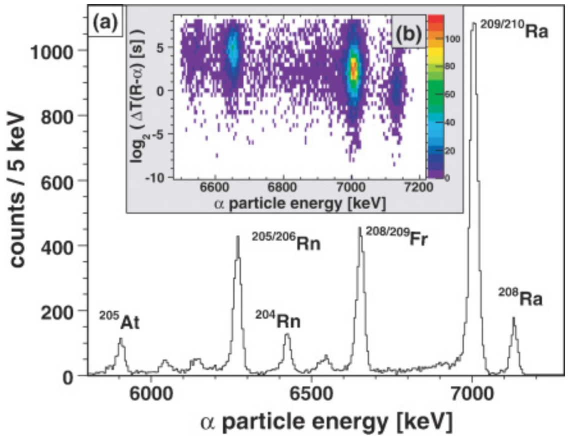


FIG. 1. (Color online) (a) Total $\alpha$-particle energy spectrum measured at the focal plane. (b) A logarithmic plot of the time difference between position-correlated $\alpha$-particles and recoils as a function of $\alpha$-particle energy.

evaporation residue and its subsequent position-correlated $\alpha$ decay as a function of the correlated $\alpha$ particle energy. Values of 4.71(8) and 4.0(1) s were obtained for the half-lives of the lower ($^{209}$Ra) and upper ($^{210}$Ra) parts of this doublet which is in good agreement with [4]. In order to maximize the statistics for subsequent analysis, the recoils were initially not alpha correlated.

Delayed decay from isomeric states in the transported ERs were searched for in the array of seven germanium detectors. In Fig. 2(a) the time difference between recoil and $\gamma$ ray detection is plotted as a function of the $\gamma$-ray energy on an event-by-event basis. At rather short times after ER implantation ($\Delta T < 16$ $\mu$s) transitions depopulating a known isomer in $^{210}$Ra [7,8] were observed. Additional lines at later times are also observed and have been highlighted by the vertical (red) boxes. A background-subtracted energy projection of this matrix for $\gamma$-rays detected between 16 ($2^4$) and 600 $\mu$s ($2^{9.25}$) is shown in Fig. 2(b). In addition to the radium $K$ x-rays, the spectrum is dominated by the 238.4(5)- and 644.4(5)-keV lines. In Fig. 2(c) the decay time of the 644-keV transition is projected onto the time axis. Assuming a single decay component for both the 644-keV transition and the background, this $\gamma$ ray is associated with the decay of a state with $t_{1/2} = 115(7)$ $\mu$s. The apparent half-life for the weaker 238-keV line was measured to be 88(31) $\mu$s.

In Fig. 3(a) a similar time versus energy plot for conversion electrons, measured in the up–stream tunnel of four Si detectors, is shown. Two broad lines are visible for $\sim$16 $\mu$s $< \Delta T <$ 600 $\mu$s. A background subtracted energy projection of conversion electrons detected within these limits is presented in Fig. 2(b). The energy spacing between the two dominant peaks corresponds to the difference between the $K$ and $L$ binding energies in radium. The peak labeled $K$ has an energy of 131 keV which is in good agreement with that expected for a K-converted 238-keV transition in Ra: 238–104 [EB(K)]–$\Delta$ keV, where $\Delta$ is the energy loss in the implantation detector. While there maybe some evidence of the $K$-converted 644-keV transition in the higher energy portion of Figs. 3(a) and (b), the $L$-converted line does not appear above the

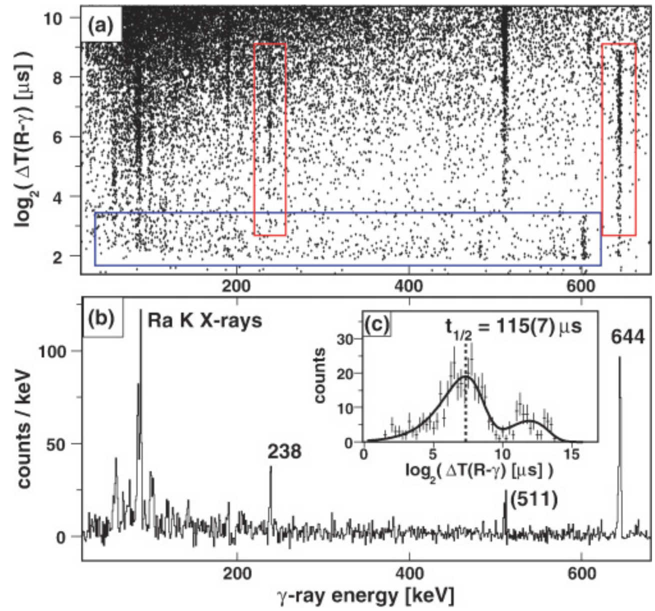


FIG. 2. (Color online) (a) A logarithmic plot of the time difference between recoil and $\gamma$ ray detection [$\log_2(\Delta T(R-\gamma))$] as a function of $\gamma$-ray energy. The horizontal (blue) box highlights transitions depopulating a known isomer in $^{210}$Ra. The vertical (red) boxes indicate the positions of two unknown decays. (b) $\gamma$-ray transitions observed between 16 and 600 $\mu$s after a recoil implantation. A fraction of the $\gamma$ rays observed later than 600 $\mu$s have been subtracted. Transition energies are labeled in keV. (c) A fit to the apparent life-time of the 644-keV $\gamma$ ray.

background fluctuations. The half-life of the 238-$KLM$ conversion electrons has been determined to be 118(6) $\mu$s, the fit is shown in Fig. 3(c).

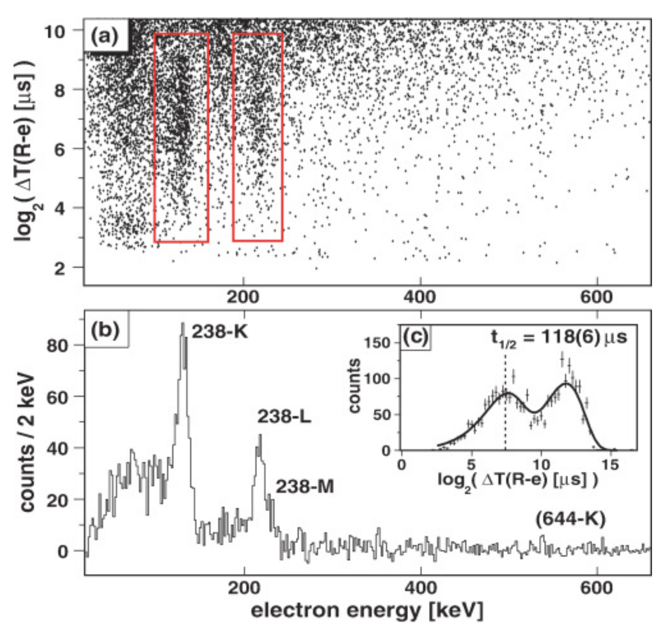


FIG. 3. (Color online) (a) and (b): same as Fig. 2 except for conversion electrons. (c) A fit to the apparent life-time of the 238-$K$ and 238-$LM$ conversion electrons.

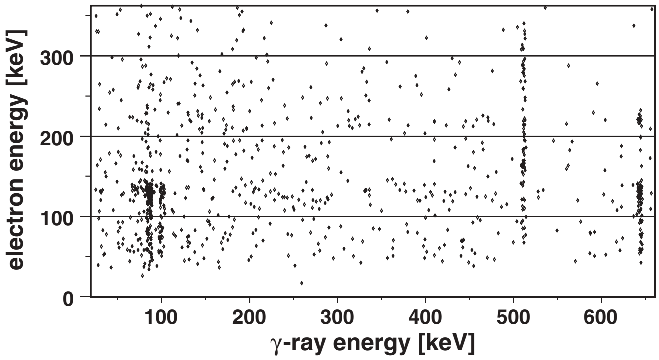


FIG. 4. A prompt coincidence matrix of conversion electrons and $\gamma$-rays [$\Delta T(e-\gamma) \leqslant 2\ \mu$s] which were detected between 16 and 600 $\mu$s of a recoil implantation.

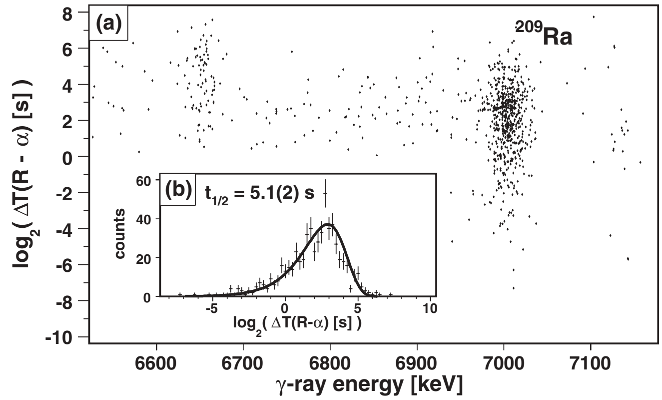


FIG. 5. (a) Decay time as a function of energy for position correlated $\alpha$ particles in coincidence with either the isomeric 644-keV $\gamma$-ray, or, the 238-$KLM$ conversion electron decay. (b) A fit to decay time of the most intense isomer-tagged recoil-correlated $\alpha$ particle.

In view of the similarity of the half-lives measured for the 644-keV $\gamma$ ray and the 238-$KLM$ conversion electrons, a matrix was constructed for $\gamma$ rays and electrons observed in prompt coincidence of one another ($\Delta T \leqslant 2\ \mu$s) and within 16–600 $\mu$s of the implantation of a recoil. This matrix, displayed in Fig. 4, clearly shows that the 644-keV gamma line is in coincidence with the 238-$K$ and 238-$LM$ conversion electrons. The coincidence between the 238-$K$ conversion electrons and the radium $K$x-rays is also evident. In an $E_\gamma$-$E_\gamma$ matrix, constructed with similar time conditions, the only coincidences observed are between the 644-keV and 238-keV transitions (two counts) and between the 644-keV line and the radium $K$ x-rays (14 counts). We therefore conclude that the 238- and 644-keV transitions form a two-step cascade that depopulates an isomeric state with a half-life of 117(5) $\mu$s.

Given that the absolute efficiencies for detecting $\gamma$ rays and electrons have been measured for the GABRIELA setup, internal-conversion coefficients could be extracted. For the 238-keV transition, the measured intensities of $I_\gamma(238) = 96(10)$ and $I_e(238:K) = 746(27)$ results in a conversion coefficient of $\alpha_K(238) = 4.0(5)$ in excellent agreement with the tabulated theoretical values for an $M2$ transition [9], see Table I. For the 644-keV transition the limit $\alpha_K(644) < 2.8(6) \times 10^{-2}$ is obtained from the measured intensities of $I_\gamma(644) = 268(16)$ and $I_{ICE}(644:K) < 20(4)$. With the additional constraint that no significant L-conversion electron peak was seen then the nature of the 644-keV transition is assigned as either an $E1$ or an $E2$.

Shown in Fig. 5(a) are the position correlated $\alpha$-particles observed in coincidence with either the delayed 644-keV $\gamma$-ray or the 238-$KLM$ conversion electrons delimited by the vertical boxes in Figs. 2(a) or 3(a), respectively. The most intense cluster has an energy $E_\alpha = 7005(4)$ keV and a FWHM = 26 keV. The inset, Fig. 5(b), shows a fit to the half-life of this $\alpha$-particle for which a value of $t_{1/2} = 5.1(2)$ s was obtained. These values agree with the accepted values for $^{209}$Ra [5], and since no $\alpha$ energy condition has been applied, Fig. 5(a) therefore indicates that the isomeric state can be attributed to $^{209}$Ra. Additionally, during a commissioning run of GABRIELA the $^{174}$Yb($^{40}$Ar, $xn$) reaction was also used, albeit, at the lower beam energy of 182 MeV [3], and, while the known $I^\pi = 8^+$ isomer in $^{210}$Ra was strongly populated no evidence of a delayed 644-keV $\gamma$ ray was seen. Furthermore, in Ref. [7] no mention of a long-lived isomer in $^{210}$Ra is made despite the experimental setup being sensitive to isomers with half-lives up to ~130 $\mu$s [10].

Our assignment of the newly observed isomer to $^{209}$Ra affirms the observation of a 644-keV transition in both prompt and delayed ($\Delta T < 6\ \mu$s) spectroscopy performed with the SASSYER separator which was assigned to the depopulation of the first excited state in $^{209}$Ra [8]. With this additional information we place the 238-keV transition above the 644-keV line.

In Fig. 6 the systematics of low-lying $13/2^+$ isomeric decays involving an $M2$ transition as part of a two-step

TABLE I. Experimental and theoretical [9] $K$- and total $L$-conversion coefficients for 238- and 644-keV transitions in radium.

| | Conversion coefficients | | | | | | |
|---|---|---|---|---|---|---|---|
| | Experiment | Theoretical | | | | | |
| | | $E1$ | $E2$ | $E3$ | $M1$ | $M2$ | $M3$ |
| $\alpha_K(238)$ | 4.0(5) | $4.8 \times 10^{-2}$ | $1.1 \times 10^{-1}$ | $2.8 \times 10^{-1}$ | 1.1 | 3.8 | 9.7 |
| $\alpha_K(644)$ | $<2.8(6) \times 10^{-2}$ | $5.9 \times 10^{-3}$ | $1.6 \times 10^{-2}$ | $3.7 \times 10^{-2}$ | 7.3 | $1.8 \times 10^{-1}$ | $3.6 \times 10^{-1}$ |
| $\alpha_K/\alpha_L(644)$ | >3 | 6.0 | 3.3 | 1.8 | | | |

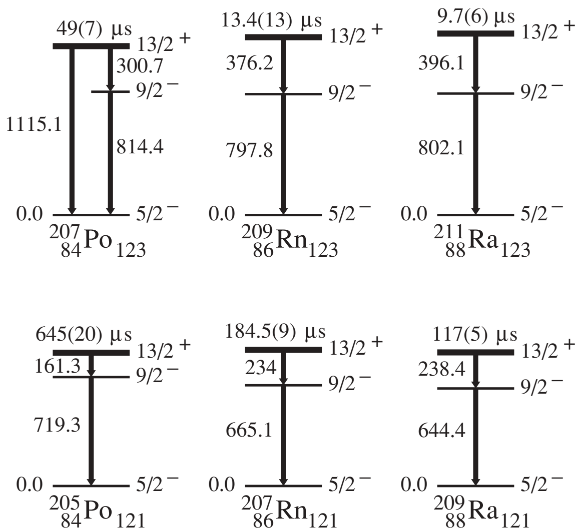


FIG. 6. Comparison of the decay of isomeric $13/2^+$ states in $N = 121$ and $N = 123$ isotones. The indicated half-lives are taken from Refs. [11] for $^{207}$Po; [12] for $^{209}$Rn; [3] for $^{211}$Ra and $^{207}$Rn; [13] for $^{205}$Po, and this work for $^{209}$Ra.

cascade, in nuclei neighboring $^{209}$Ra, is presented. In view of similarity of the decay pattern of the new isomer observed in $^{209}$Ra and these systematics we assign the $^{209}$Ra$^m$ state to an $I^\pi = 13/2^+ \nu(i_{13/2})^{-1}$ excitation. The Weisskopf hindrance factor of 680 for the delayed $M2$ transition in $^{209}$Ra agrees well with the values calculated for other $I_i = 13/2^+ \rightarrow I_f = 9/2^-$ transitions of the same type.

Delayed spectroscopy of $^{209}$Ra, using the GABRIELA detection system at the focal plane of VASSILISSA, has revealed a low-lying $I^\pi = 13/2^+$ isomeric state. The $M2$ nature of the decay from this state has been determined from combined $\gamma$-ray and internal conversion electron spectroscopy. The half-life of this state has been measured to be 117(5) $\mu$s.

The GABRIELA project is jointly funded by JINR (Russia) and IN2P3/CNRS (France). Work at FLNR was performed partially under the financial support of the Russian Foundation for Basic Research, Contract no. 08-02-00116 and JINR-BMBF (Germany), JINR-Polish, JINR-Slovak Cooperation Programmes. Financial support from the Norwegian Research Council and the Bulgarian National Science Fund (Contract no. 204/06) is acknowledged.

[1] A. V. Yeremin *et al.*, Nucl. Instrum. Methods Phys. Res. B **126**, 329 (1997).
[2] O. N. Malyshev *et al.*, Nucl. Instrum. Methods Phys. Res. A **440**, 86 (2000).
[3] K. Hauschild *et al.*, Nucl. Instrum. Methods Phys. Res. A **560**, 388 (2006).
[4] K. Valli, W. Treytl, and E. K. Hyde, Phys. Rev. **161**, 1284 (1967).
[5] L. P. Ekström and R. B. Firestone, WWW Table of Radioactive Isotopes, database version 2/28/99 from URL http://nucleardata.nuclear.lu.se/nucleardata/toi/
[6] F. G. Kondev, Nucl. Data Sheets **108**, 365 (2007).
[7] J. F. C. Cocks *et al.*, J. Phys. G **25**, 839 (1999).
[8] J. J. Ressler *et al.*, Phys. Rev. C **69**, 034331 (2004).
[9] T. Kibédi, T. W. Burrows, M. B. Trzhaskovskaya, and C. W. Nestor, Jr., AIP Conf. Proc. **769**, 268 (2005); URL http://wwwrsphysse.anu.edu.au/nuclear/bricc
[10] K. Hauschild *et al.*, Phys. Rev. Lett. **87**, 072501 (2001).
[11] M. J. Martin, Nucl. Data Sheets **70**, 315 (1993).
[12] A. R. Poletti *et al.*, Nucl. Phys. **A440**, 118 (1985).
[13] F. G. Kondev, Nucl. Data Sheets **101**, 521 (2004).